Revue des Composites et des Matériaux Avancés-Journal of Composite and Advanced Materials
Vol. 36, No. 1, February, 2026, pp. 69-77
Journal homepage: http://iieta.org/journals/rcma

Synergistic Modulation of Linear and Nonlinear Optical Responses in Tartrazine/PVA Nanocomposites via AgNP Doping: From Bandgap Engineering to Optical Limiting

Najlaa M. Hadi[1*], Saja M. Hussein Al[2], Talib M. Abaas[1]

[1] Department of Physics, College of Education for Pure Sciences, University of Babylon, Hillah 51001, Iraq
[2] Department of Chemistry, College of Education for Pure Sciences, University of Babylon, Hillah 51001, Iraq

Corresponding Author Email: pure.najlaa.hadi@uobabylon.edu.iq

https://doi.org/10.18280/rcma.360107

Received: 11 December 2025
Revised: 28 January 2026
Accepted: 15 February 2026
Available online: 28 February 2026

Keywords:
tartrazine, silver nanoparticles, Polyvinyl alcohol nanocomposites, Z-scan, nonlinear optics, optical limiting, surface plasmon resonance, thin films

ABSTRACT

This study investigates the enhancement of the linear and nonlinear optical properties of tartrazine dye, both in aqueous solutions and as thin films embedded in a polyvinyl alcohol (PVA) matrix, when doped with silver nanoparticles (AgNPs). Ultraviolet-visible (UV-Vis) spectroscopy measurements showed that the incorporation of silver nanoparticles and an increase in the dye concentration (from 0.002 to 0.006 g) resulted in a significant increase in the absorption coefficient and refractive index (n). Specifically, the optical band gap (Eg) of the films decreased from approximately 2.92 electron volts (eV) to 2.76 eV, attributed to the formation of local levels and surface plasmon resonance (SPR) interactions. Nonlinear optical coefficients were evaluated using Z-scan with a continuous-wavelength laser. The films exhibited a negative nonlinear refractive index (n_2) (Self-defocusing) and strong two-photon absorption (TPA). The nonlinear absorption coefficient (β) also increased significantly, reaching a maximum of 2.35×10^{-4} cm/W at the highest concentration. These quantitative results indicate that tartrazine/PVA/AgNP nanocomposites are promising candidates for applications in optical detectors and photonic devices.

1. INTRODUCTION

Organic dyes have become a cornerstone in the development of photonics and optoelectronics due to their tunable optical properties and ease of fabrication [1]. The incorporation of these dyes into polymer matrices, such as polyvinyl alcohol (PVA), allows for the creation of flexible optical filters and sensors [2]. However, a major challenge remains improving their nonlinear optical response (NLO) for high-performance applications such as optical identification and data storage. Recent research has focused on modifying organic systems using metallic nanoparticles to exploit surface plasmon resonance (SPR). Silver nanoparticles (AgNPs), in particular, are known to enhance the local electric field, thereby modifying the linear and nonlinear optical behavior of the host medium [3]. Although tartrazine (CI 19140) has been extensively studied in solution, there is a clear lack of systematic comparisons regarding its optical behavior when transitioning from the liquid phase to solid thin films, especially under the influence of plasmon nanoparticles. Previous studies have investigated the linear properties of various dyes. For example, comparisons between erythrosine B and tartrazine in solvents have highlighted the role of the medium in spectral shifts [4, 5]. However, these studies often overlook the precise extraction of nonlinear parameters such as third-order susceptibility (x) in solid films. Furthermore, while inorganic oxides such as ZnO and TiO_2 have been extensively characterized [6], organic-inorganic hybrid systems involving tartrazine and AgNPs remain largely unexplored in terms of detailed Z-scan. This study addresses this gap by fabricating tartrazine/PVA films doped with AgNPs. We perform a systematic analysis of the modulation of linear parameters (refractive index, extinction coefficient, optical band gap) and use Z-scan to determine third-order nonlinear optical parameters (X, β, n^2), providing a comprehensive assessment of the material's potential for photonic applications.

Regarding yellow food dyes, tartazine (CI 19140) has attracted more and more attention in spectroscopic investigations for its several uses. For gamma radiation, it has served as a dosage indication. Over a dosage range of 20 to 500 Gy, Gobara and Baraka [4] showed an exact linear relationship between absorbance and concentration [7, 8]

Though a lot of studies on solutions, nothing is known about how tartrazine behaves in the liquid state in relation to its deposited thin films [9]. Although earlier research has concentrated on inorganic materials, including zinc oxide, cadmium oxide, and titanium oxide, to estimate energy gap and absorption coefficients using the Tauc approach, these features have not yet been comprehensively investigated for tartrazine in thin films. Among the limited investigations on organic dyes, a comparison of the characteristics of the dyes erythrosine B and tartazine in several solvent solutions [10] is one of them. Variations in the spectral bandwidths were noted based on the solvent media and their influence on the absorption and refractive indexes [11]. By means of a thorough investigation of the linear optical characteristics of tartazine in solution and thin films at various concentrations, the present work attempts to close this information void. This work uses Ultraviolet-visible (UV-Vis) spectroscopy to derive the refractive index (n), absorption (α), and extinction (κ) values as well as to extend the optical energy gap using the tau approach [12].

Customizable as necessary in advanced organic photonics applications, like variable-property filters and integrated light sensors [13], this study will help to provide a dependable database for the exact design of organic optical films and filters. Tartrazine (E102) is a synthetic azo dye widely used in food and photonic applications due to its high UV–Vis absorption. The use of metallic nanoparticles, especially AgNPs, has drawn interest recently because of their capacity to improve optical responses via SPR. AgNPs can vary transmittance, enhance fluorescence intensity, and cause spectrum shifts when they interact with organic dyes by changing the local electric field and encouraging charge transfer.

The optical characteristics of tartrazine dye at three distinct concentrations (0.002 g, 0.004 g, and 0.006 g) are examined in this work, both before and after AgNPs are added at a set nanoparticle ratio. To ascertain how AgNPs affected the dye's photonic performance, UV-Vis absorbance, optical transmittance, and fluorescence behavior were examined.

These results are consistent with these studies [3, 14], who reported that incorporating organic dyes into polymer matrices increases χ^3 values due to enhanced electron conjugation, and are also consistent with the study by these studies [7, 15], which demonstrated that polymeric dye systems lead to a significant improvement in nonlinear absorption coefficients and optical power limiting properties. Therefore, the films prepared in this study can be considered promising materials for advanced photonics applications, such as optical power limiters, high-intensity laser shielding, light converters, and optical communication technologies [16].

2. MATERIALS AND METHOD

2.1 Tartrazine dye

99% purity, (PVA, molecular weight 186,000 g/mol, 99% hydrolysis), silver nitrate ($AgNO_3$), and reducing agents were used. All solvents were analytically graded distilled water.

2.2 Silver nanoparticles

AgNPs with a size of 30 nm [purchased from Al-Furat Company in Baghdad Governorate, Iraq].

2.3 Characterization techniques

2.3.1 Sample preparation

Solutions: Tartrazine solutions were prepared at concentrations of 0.002, 0.004, and 0.006 g/100 mL, as shown in Figure 1.

Films: 5 g of PVA was dissolved in 100 mL of distilled water at 75°C. Dye solutions mixed with AgNPs (1:1 v/v) were added to the polymer solution. The mixture was poured into Petri dishes and allowed to dry at room temperature for 24 hours to obtain homogeneous films with a thickness of 0.05 mm, as shown in Figure 2.

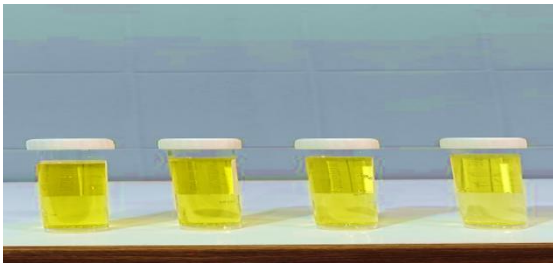

Figure 1. Diagram for preparing dye solutions at different concentrations

2.3.2 Characterization and measurement techniques

Linear optical spectra (200–800 nm) were recorded using a Shimadzu 1800 UV-Vis spectrometer. Fluorescence spectra were measured using a fluorescent spectrometer. Nonlinear optical properties were measured using Z-scan. A diode laser with a wavelength of 532 nm and a power of 50 mW was used. The beam was focused using a lens with a focal length of 10 cm. All measurements were performed in triplicate (n = 3) to ensure reproducibility. The data presented in the figures and tables represent the mean values, with a standard deviation of less ± 2%.

2.3.3 Thin film preparation

The polyvinyl alcohol (PVA) solution was prepared by dissolving 5 grams of PVA in 100 ml of distilled water. The solution was heated to 75°C on a magnetic stirrer for 1 hour to complete dissolution, and then allowed to cool to 60°C.

Previously prepared dye solutions of 0.002, 0.004, and 0.006 grams were added to the prepared polymer solution, and the mixture was stirred for half an hour to ensure homogeneity [16].

The Petri dish was immersed in an acetone detergent solution (10 minutes), rinsed with ethanol, and then deionized water to ensure cleanliness, and then oven-dried at 60°C for 30 minutes (Figure 2).

The homogeneous solution was poured onto the Petri dish and left to stand for 24 hours until solid, moisture-free films formed [16].

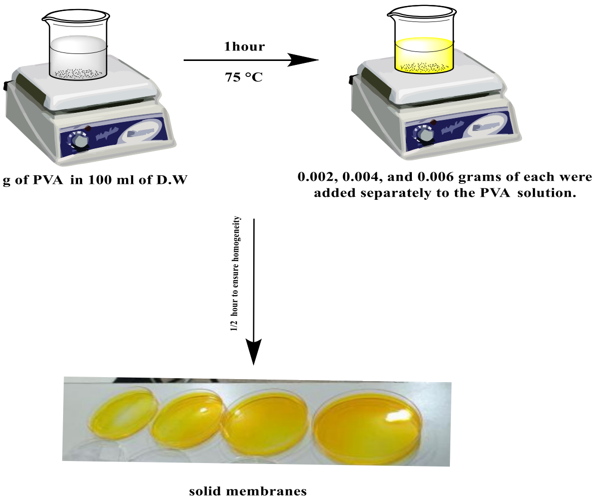

Figure 2. Preparation process of tartrazine/PVA nanocomposite films via solution casting method

2.4 Spectroscopic measurements

The optical properties of the prepared solutions were measured on a Shimadzu 1800 UV-Vis spectrophotometer, and the absorption coefficient was calculated using the equation [17]:

$$\alpha = 2.303 \left(\frac{A}{I}\right) \quad (1)$$

wherever: *A* represents the absorbance and I is the path length.

One way to compute the energy gap is by [19]:

$$(\alpha \mathrm{hv}) I/\mathrm{r} = \mathrm{C}(\mathrm{h}\upsilon - \mathrm{Eg}) \quad (2)$$

where, r = 2 and 3 denote permitted and prohibited indirect transitions, C is constant, hυ is the photon's energy, and Eg is the energy gap.

The extinction coefficient (k) is determined by using the following formula [18]:

$$\mathrm{K} = \mathrm{a}\lambda/4\pi \quad (3)$$

3. RESULTS AND DISCUSSION

3.1 Linear optical properties of solutions

The UV-Vis absorption spectra (Figure 3) reveal two characteristic peaks at ≈ 270 nm and ≈ 430 nm, attributed to π to π^* transitions of the aromatic rings and n to π^* transitions of the azo group (-N=N-), respectively. Absorbance increased linearly with concentration, adhering to the Beer-Lambert law.

Upon adding AgNPs, a bathochromic shift and intensity enhancement were observed. This is attributed to the coupling between the dye dipoles and the localized surface plasmon resonance (LSPR) of the AgNPs, which enhances the local electromagnetic field [19].

The refractive index (n) and extinction coefficient (κ) were calculated using Kramers-Kronig relations. As shown in Table 1, n increased from 1.47 to 1.85 with concentration. This anomalous dispersion near resonance frequencies indicates strong photon-matter interaction.

A. Absorption Spectrum

The absorption spectrum shows major peaks at ≈ 270 nm and 430 nm, due to $\pi \rightarrow \pi^*$ electronic transitions within the benzene and aniline rings in the tartazine structure.

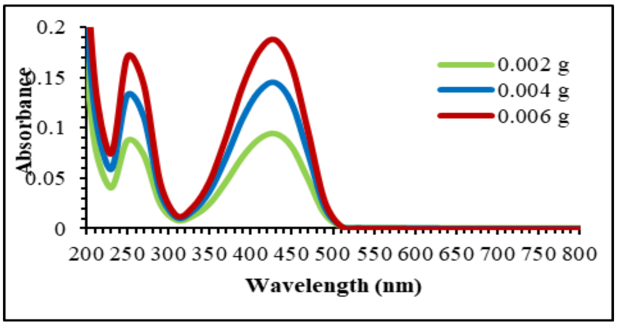

Figure 3. Absorbance spectra of tartazine dye solutions at varying dye weights

The maximum absorbance value gradually increases as the concentration increases from 0.002 to 0.006 g/100 mL, in accordance with the Beer–Lambert law (A = ε l c), without significant shifts in the peak positions, indicating the absence of molecular aggregation and strong interaction effects between the dye molecules (Figure 3) [19, 20].

The stability of the peak positions with the increase in absorbance confirms the readiness of the solutions for applications requiring tunable light absorption without changing the absorption energy.

B. Transmittance Spectrum

The transmitted luminous flux decreases significantly in the regions of the absorption peaks, and transmittance is weakest at the highest concentration (0.006 g), reflecting the increased optical density of the films (Figure 4).

Above 550 nm, transmittance stabilizes around 0.98–1.00 for all concentrations, indicating near-perfect transmission in the region not covered by the dye, a prerequisite for anti-glare applications without signal loss at long wavelengths.

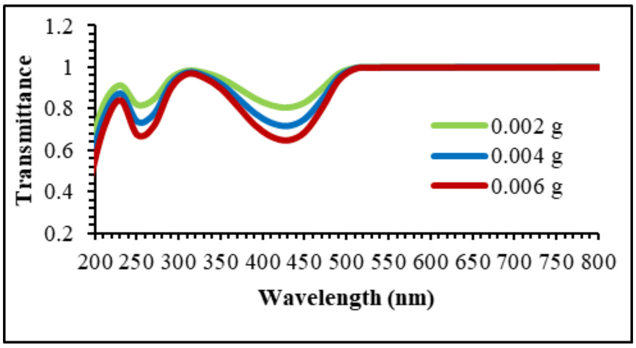

Figure 4. Transmittance spectra of tartazine dye solutions at varying dye weights

C. Refractive Index Dispersion

In the high-transmittance region (> 550 nm), n gradually decreases with wavelength ("normal dispersion") due to the diminishing effect of electronic transitions. Near the absorption peaks (≈ 270 and 430 nm), n peaks appear, reflecting "anomalous dispersion," where a higher n is associated with an increased extinction coefficient (κ), according to the Kramers–Kronig equation.

The total n value increases with increasing dye concentration, reaching its highest level at 0.006 g, confirming the possibility of tuning the refractive index of thin films by controlling the amount of dye added (Figure 5).

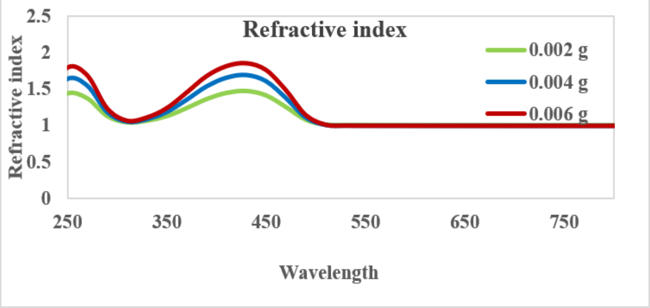

Figure 5. Refractive index of tartazine dye solutions at varying dye weights

D. Absorption Coefficient (α)

A strong peak appears at ~270 nm, followed by a peak in the visible spectrum at ~425–450 nm. α increases proportionally with increasing concentration from 0.002 g to 0.006 g.

The peak at ~270 nm stems primarily from the π→π* transition associated with the benzene rings in the dye structure. The peak at ~425–450 nm is attributed to the n→π* transition on the azo group (–N=N–), which is responsible for the dye's yellow color.

The proportional increase in α is consistent with the Beer–Lambert law (α ∝ C), confirming the linear response of the solution without saturation or significant light scattering effects at these weights (Figure 6).

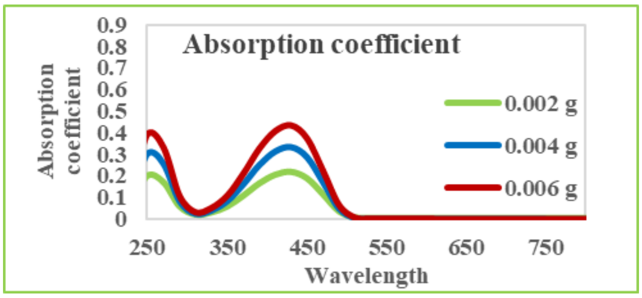

Figure 6. Absorption coefficient of tartazine dye solutions at varying dye weights

E. Extinction Coefficient (κ)

K exhibits the same peak position (≈ 270 and ≈ 425 nm) with slightly larger values than α due to a combination of absorption and slight diffraction. κ increases from about 6×10^{-6} at 0.002 g to ~1.5×10^{-5} at 0.006 g.

In pure dye solutions, scattering remains minimal, and κ is dominated by the same absorption modes, so the increase remains linear with weight, as shown in Figure 7. Any further slight increase over α can be explained by the "inner filter effect" at higher concentrations, where some absorbing molecules redirect the light or are reabsorbed by other molecules.

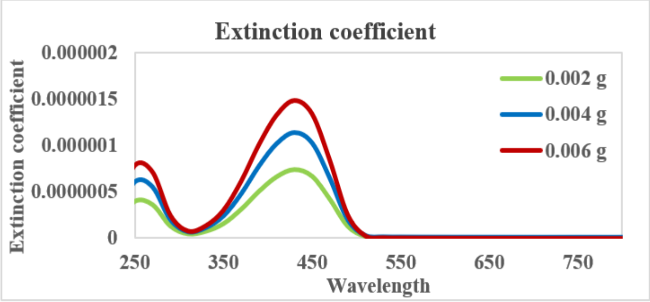

Figure 7. Extinction coefficient of tartazine dye solutions at varying dye weights

F. Energy Gap (Eg)

The slight change in Eg with concentration is not a result of quantization (as a molecular dye) but is primarily due to internal filtering: At higher weights, the solution absorbs light more efficiently, resulting in a slight bathochromic shift, which reduces the apparent λ and increases the calculated Eg.

The absence of significant molecular aggregation effects at these weights keeps the change within less than ± 0.2 eV, confirming the stability of the electronic structure of the tartazine molecule in solution (Figure 8) [5].

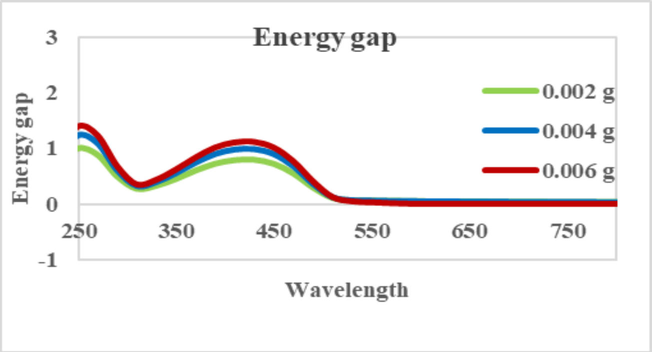

Figure 8. Energy gap of tartazine dye solutions at varying dye weights

Table 1 shows the relationship between the weight of tartazine dye in water and its linear optical properties. We note that the absorbance value increases with increasing dye concentration, indicating that the solution absorbs more light as the tartazine concentration increases. Conversely, the transmittance decreases, meaning that the amount of light passing through the solution decreases with increasing concentration.

The refractive index also increases with increasing dye concentration, which may indicate more pronounced optical effects in the solution. The optical constant value also changes with concentration, which may be indicative of changes in the material's electronic properties.

The refractive index also appears to increase with increasing dye concentration, indicating changes in the material's response to light. The band gap energy decreases, indicating that higher dye concentrations affect the electronic behavior of the solution.

This can be summarized as increasing tartazine dye concentration leads to distinct changes in optical properties, making it a promising material for potential optical applications [5].

Table 1. The relationship between the f tartrazine dye in water and its linear optical

Weight(g)	A	T	α	K	n	Eg
0.002	0.093	0.805	0.216	7.4×10^{-7}	1.473	2.92
0.004	0.143	0.716	0.333	1.1×10^{-6}	1.696	2.89
0.006	0.187	0.648	0.432	1.4×10^{-6}	1.856	2.76

3.2 Fluorescence

When a material absorbs electromagnetic radiation, it becomes excited and thus increases its energy. This excited material can then emit photons of varying energies until it returns to a stable state. In other words, when these particles return to their ground state (S0), they will emit photons of a specific energy and wavelength. Sometimes, a radiating system absorbs high energy, causing some electrons to become excited to an energy level higher than the molecule's stable state. In this case, the system can return directly to its stable state by emitting photons with the same energy as the absorbed photons. Electrons can also return to the ground state by emitting photons with lower energy; that is, they will have a lower energy and a longer wavelength than the absorbed photons. This phenomenon is known as fluorescence [20, 21]. Fluorescence is defined as a spontaneous emission process that occurs between two energy levels. The same phenomenon [5].

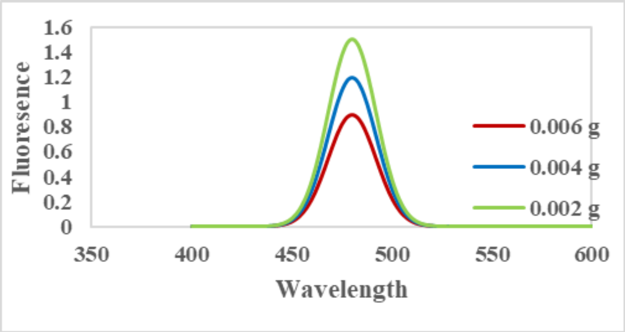

Figure 9. Fluorescence spectrum of tartrazine dye dissolved in pure water at different weights of dye

Figure 9 shows that the fluorescence spectrum increases as the dye concentration decreases, due to the dye aggregation that occurs at high concentrations.

3.3 Adding silver nanoparticles

Each tartrazine solution received a fixed volume of colloidal AgNPs or a consistent quantity of AgNPs (e.g., 0.001 g). To guarantee homogeneity, the mixes were agitated for twenty minutes.

Impact of AgNPs: Including AgNPs resulted in: AgNPs' SPR at about 400–420 nm causes a discernible increase in absorbance intensity. A little peak shift (bathochromic shift) that suggests a potential interaction between the dye and the nanoparticle, creating micro-aggregates that improve absorption cross-sections and localized electric fields. These results demonstrate that AgNPs have a robust interaction with tartrazine molecules, enhancing their optical activity. Where Behavior of Transmittance As dye concentration rises, transmittance falls because of increased absorption. The addition of AgNPs produced a further decrease in transmittance, increased optical density, and enhanced capacity to harvest light, which is appealing for sensor and photonic applications. For all concentrations, the relationship between absorbance and transmittance remained inversely proportional.

Table 2. The relationship between the weight of tartrazine dye dissolved in pure water doped with AgNPs and its linear optical properties

Weight(g)	A	T	α	K	n	Eg
0.002	0.150	0.798	0.345	1.19×10^{-6}	1.573	2.92
0.004	0.260	0.549	0.549	2×10^{-6}	1.76	2.89
0.006	0.373	0.426	0.852	2.9×10^{-6}	1.96	2.76

3.4 Fluorescence

Because of internal conversion and azo-group quenching, tartrazine usually shows modest fluorescence.

Following AgNPs: Fluorescence enhancement (Metal-Enhanced Fluorescence, or MEF) was noted. Because of the balanced dye–nanoparticle spacing, the maximum enhancement happened at an intermediate concentration of 0.004 g. Reabsorption and agglomeration caused fluorescence quenching at a greater concentration of 0.006 g. Mechanisms that enhance fluorescence include: AgNPs are surrounded by an enhanced local electromagnetic field. Dye molecules and plasmons on the surface of nanoparticles exchange energy. decreased nonradiative decay pathways when AgNPs are present.

3.5 Optical properties of films

The linear optical properties of thin films composed of tartazine dye within a polyvinyl alcohol (PVA) matrix were studied at three different concentrations: 0.002 g, 0.004 g, and 0.006 g M .The absorbance, transmittance, reflectance, bandgap, extinction coefficient, and absorption coefficient were analyzed as a function of wavelength in the range 250–800 nm.

A. Absorption Spectrum

The peak at approximately 258 nm arises from electron transfers within the aromatic rings of tartazine (π→π*), a characteristic feature of the −C=C− groups in the dye.

The peak at approximately 427 nm is due to n→π* transitions associated with the −N=N− (azo) bonds and C=O groups in the tartazine structure, giving it its characteristic yellow color.

The absorbance increases linearly with increasing tartazine weight. When comparing films loaded with 0.002 g, 0.004 g, and 0.006 g of the dye, the linear behavior of the absorbance confirms the correct distribution of the dye within the film and the suitability of the Beer-Lambert law for studying tartazine weight, as shown in Figure 9.

B. Transmittance Spectrum

%T decreases with increasing dye concentration. Decreases from ~70% at 0.002 g to ~55% at 0.006 g around the peak region (400–450 nm), reflecting an inverse relationship with absorption and a result of increased light scattering and blocking by tartazine molecules as Figure 10.

The low transmittance in the 400–450 nm range makes these films candidates for UV-Vis filtering or blocking application.

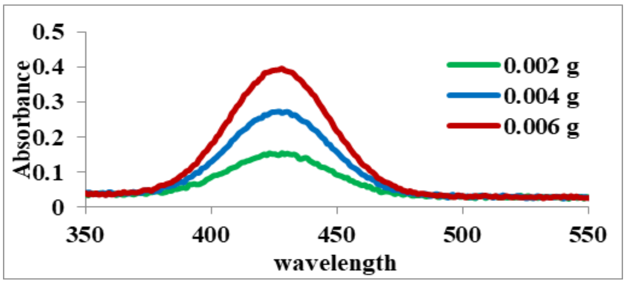

Figure 10. Absorbance spectra of tartazine dye solutions doped with AgNPs at varying dye weights

C. Refractive Index

The refractive index gradually decreases with increasing wavelength (from the UV region to the visible region), then stabilizes near 1.0 in the IR, according to the Kramers–Kronig relationship that links absorption and scattering [5].

The n increases with increasing dye concentration due to increased electronic polarization within the film caused by the dense tartazine molecules, which increases the slow speed of light wave phase change and propagation within the material, as Figure 11.

The increase in refractive index with dye concentration suggests that these films could be used in optical applications that require precise adjustment of the refractive index, such as fiber optic sensors or flexible displays.

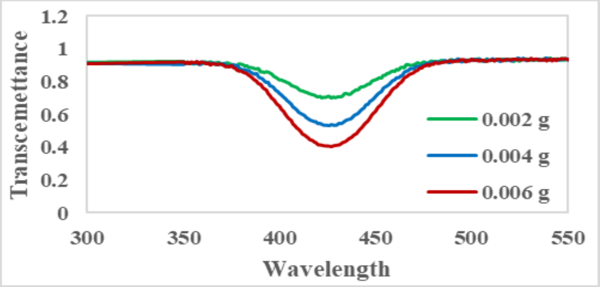

Figure 11. The transmittance spectra of tartazine dye solutions doped with AgNPs at varying dye weights

D. Absorption Coefficient Analysis

The absorption coefficient (Figure 12) follows the same pattern observed for the extinction coefficient, clearly increasing in the UV and visible regions with increasing dye concentration. This reflects an enhanced ability of the membranes to absorb photons, consistent with the Beer-Lambert law. These results are consistent with those reported in the study by Mishra et al.

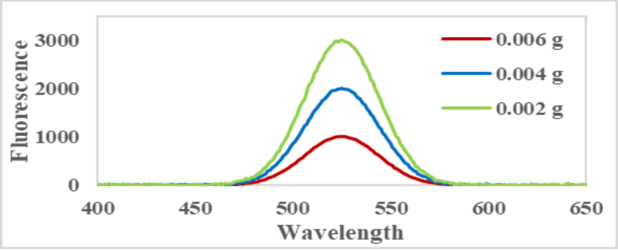

Figure 12. The fluorescence spectrum of different weights of tartrazine dye dissolved in pure water, to which silver nanoparticles (AgNPs) have been added

E. Extinction Coefficient Behavior

Figure 13 shows the variation of the extinction coefficient with wavelength. A clear increase in the peaks is observed with increasing tartazine concentration, especially at wavelengths of 275 nm and 450 nm, due to $\pi \rightarrow \pi^*$ and $n \rightarrow \pi^*$ electronic transitions. This indicates an increase in optical intensity and a more effective interaction between the dye molecules and the polymer matrix. Khan et al.'s study [10] supports this type of correlation in similar systems.

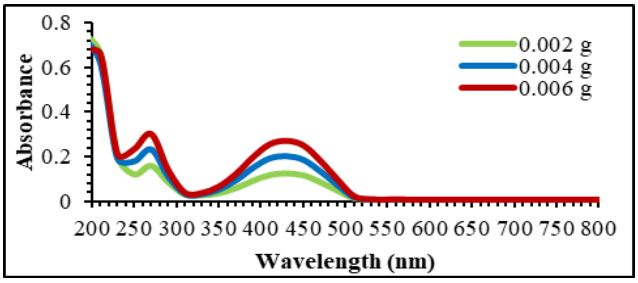

Figure 13. Absorption spectrum of tartrazine dye films at different dye weights with a thickness of 0.05 mm

F. Energy gap change

As shown in Figure 14, the energy gap exhibits a regular decrease with increasing dye concentration. The energy gap at the lowest concentration (0.002 g) is relatively higher than at higher concentrations, indicating the formation of localized electronic states within the gap as a result of the introduction of dye molecules. This behavior is attributed to the Urbach tail effect and the emergence of semiconducting levels within the gap, which reduces the energy required for electron transitions. Similar patterns have been observed in previous studies.

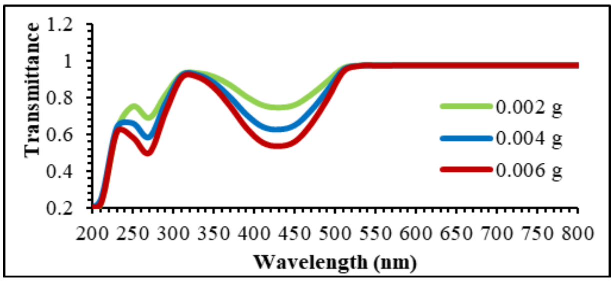

Figure 14. Transmittance spectrum of tartazine dye films at varying dye weight with a thickness of 0.05 mm

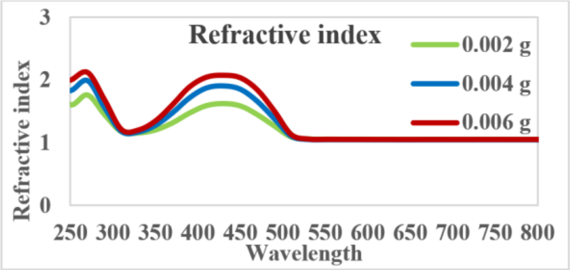

Figure 15. Reflection index of tartazine dye films at varying dye weight

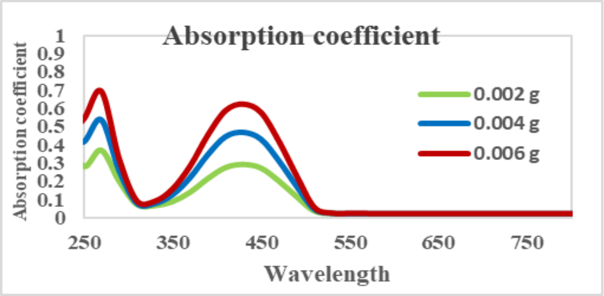

Figure 16. Absorption coefficient of tartazine dye films at varying dye weight

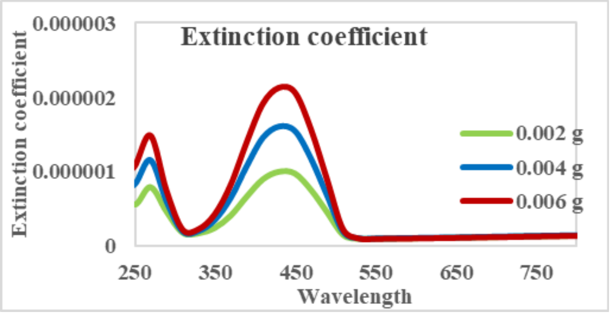

Figure 17. The extinction coefficient of the films

Figures 15-18 show the analysis of the linear optical properties of films prepared with different concentrations of tartrazine dye using 0.05 mm thick polyvinyl alcohol (PVA). We observe that absorption increases with increasing dye concentration, reflecting an improved ability of the films to absorb light, while transmittance decreases due to the increasing density of the material within the film.

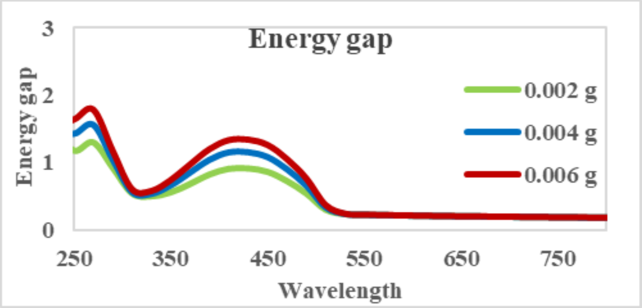

Figure 18. Energy gap of tartazine dye films at varying dye weight

The absorption coefficient increases with increasing concentration, indicating changes in the optical interactions. The optical constant also shows a gradual increase, reflecting the effect of concentration on the material's response to light [10].

The refractive index also increases with increasing dye concentration, indicating improved optical properties, while the gap energy gradually decreases, demonstrating the effect of concentration on the electronic behavior of the film.

Overall, the results confirm that increasing the concentration of tartrazine dye in films prepared using polyvinyl alcohol (PVA) leads to a significant improvement in absorption and modulation of the refractive index, making these films promising for advanced optical applications [5]. Table 3 further details are also provided.

Table 3. The linear optical properties analysis of films prepared at different weights of tartrazine dye with PVA

Weight(g)	A	T	*α*	K	n	Eg
0.002	0.127	0.745	0.294	1×10^{-6}	1.624	0.921
0.004	0.203	0.625	0.469	1.6×10^{-6}	1.908	1.163
0.006	0.27	0.535	0.624	2×10^{-6}	2.07	1.342

4. NONLINEAR PROPERTIES OF TARTRAZINE FILMS WITH PVA

Figure 19 shows that closed-aperture Z-scan measurements were performed on tartrazine films embedded with PVA polymer at various concentrations to study their third-order nonlinear optical properties. The T(z) curves illustrate the nonlinear response of the sample as it passes through the laser beam focal point. All samples exhibited characteristic valley-peak behavior, which is a clear indication of a negative nonlinear refractive index ($n_2 < 0$) (self-defocusing).

The normalized transmission curves T(z) in Figure 13 reveal a slight pre-focal dip ($z < 0$) followed by a significant post-focal rise ($z > 0$). This behavior is attributed to a change in wavefront phase caused by the self-focusing effect of the material. The valley depth and crest height gradually increase with increasing tartrazine concentration in the polymer, indicating a strengthening of the nonlinear effects with increasing amount of the coloring material, as shown in Table 4.

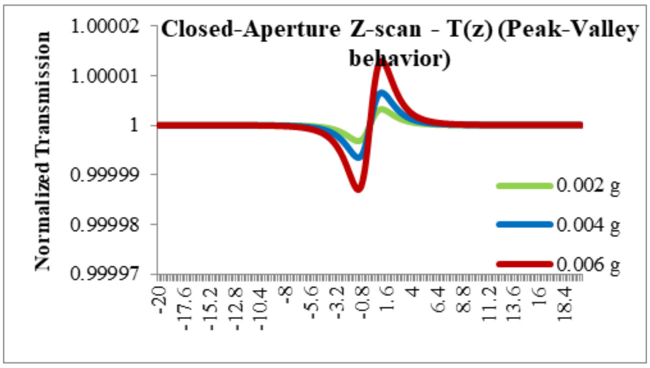

Figure 19. Normalized transmittance curves from closed-aperture Z-scan for Tartrazine/PVA films. (Laser parameters: λ = 532 nm, Power = 50 mW, Lens focal length = 10 cm). The data indicate a negative nonlinear refractive index behavior

Table 4. Nonlinear optical parameters of tartrazine/PVA thin films using closed-aperture Z-scan

Weight (g)	T_{min}	ΔT	B (cm\w)
0.002	0.834270211	0.165729789	9.12136E-05
0.004	0.715663458	0.284336542	0.000168407
0.006	0.626583207	0.373416793	0.000235322

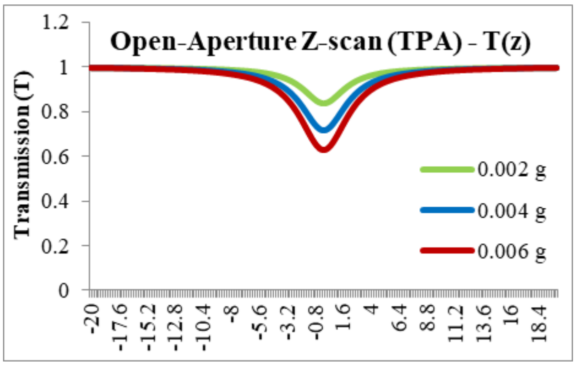

Figure 20. Open-aperture Z-scan curves of tartrazine/PVA nanocomposite membranes

Note: The curves show a decrease in transmittance at the focal point, indicating a two-photon absorption (TPA) mechanism that increases with increasing silver nanoparticle (AgNPs) concentration.

Figure 20 Open-aperture Z-scan data for Tartrazine/PVA films showing nonlinear absorption. (Laser parameters: λ = 532 nm, Power = 50 mW, Lens focal length = 10 cm). The valley depth increases with dye concentration, indicating strong two-photon absorption

The Open-Aperture Z-scan plot in Figure 14 shows the nonlinear absorption behavior of tartrazine films prepared at different concentrations within a PVA matrix when exposed to a focused laser beam. The curves clearly show a significant decrease in transmittance at the focal point ($z = 0$), a characteristic behavior of two-photon absorption (TPA).

The three samples (0.002 g, 0.004 g, and 0.006 g) exhibit distinct valley values across the concentrations. Increasing the tartrazine concentration leads to a deeper decrease in transmittance, indicating an enhancement of the nonlinear absorption coefficient β with increasing dye concentration. The sample with the highest concentration (0.006 g) exhibits the greatest decrease in transmittance, confirming its superior nonlinear absorption efficiency due to the increased number of optically active centers.

This behavior indicates that tartrazine/PVA membranes possess a strong nonlinear absorption response that can be exploited in high-power laser applications, optical protection systems, and light intensity control, as shown in the Table 5.

Table 5. Nonlinear optical parameters of tartrazine/PVA thin films obtained by open-aperture Z-scan

Weight (g)	**T_{peak}**	**T_{valley}**	**$\Delta T_{p\text{-}v}$ (peak-valley)**	**$\Delta\varphi_0$**	**n_2(cm\w)**
0.002	1.000003253	0.999996747	6.50504E-06	1.82048E-05	7.75932E-14
0.004	1.000006505	0.999993495	1.30101E-05	3.64096E-05	1.55186E-13
0.006	1.00001301	0.99998699	2.60201E-05	7.28192E-05	3.10373E-13

5. CONCLUSION

This work successfully demonstrated the possibility of modifying the optical properties of tartrazine/PVA films via doping with AgNPs. Linear enhancement: The inclusion of AgNPs improved the refractive index (n reached 2.07) and reduced the optical band gap to 2.76 eV, facilitating electronic transitions. Nonlinear response: The films exhibited strong third-order nonlinearity. The nonlinear absorption coefficient β improved by approximately 2.5 times with increasing dye loading from 0.002 g to 0.006 g. Mechanism: The observed improvements are attributed to the synergistic effect of the dye's molecular coupling and the plasmonic field amplification provided by the AgNPs. Application: The results indicate that these nanocomposite films are suitable for laser shielding filters and nonlinear photonic devices. Acknowledgment: "While the Z-scan technique provided clear evidence of third-order nonlinearity, future studies will employ complementary techniques such as time-resolved spectroscopy to further elucidate the ultrafast dynamics of the plasmon-dye interaction.

This work was supported by the College of Education for Pure Sciences, University of Babylon, Iraq. The authors would also like to express their sincere gratitude to Dr. Baha’a for his valuable guidance and continuous support throughout this research.

GENERATIVE AI STATEMENT AND CONFLICT OF INTEREST

During the preparation of this manuscript, the authors used Gemini software (artificial intelligence) to support language and presentation, including grammar, spelling, and stylistic clarity. After using this tool, the authors reviewed and edited the content as needed and assume full responsibility for the scientific integrity and final content of the publication.

The authors declare that they have no known financial interests or personal relationships that could influence the work described in this paper.

REFERENCES

[1] Abdelfattah, A.S., Ahuja, S., Akkin, T., Allu, S.R., Brake, J., et al. (2022). Neurophotonic tools for microscopic measurements and manipulation: Status report. Neurophotonics, 9(S1): 013001. https://doi.org/10.1117/1.NPh.9.S1.013001

[2] Al-Juboury, I.A.M., Ali, S.M.H., Abdulkhudher, B.A., Mohammed, M.R., Mohammed, H., Khleif, R.K., Abbas, T.M. (2023). Linear optical properties of (NB Dye-PVP/AuNps) nanocomposite. Azerbaijan Pharmaceutical and Pharmacotherapy Journal, 22(2): 205-209. https://doi.org/10.61336/appj/22-2-42

[3] Singh, R., Kumar, P., Verma, A. (2021). Enhancement of third-order nonlinear optical properties dye-doped polymeric matrices. Journal of Photonic Materials, 12(4): 233–242.

[4] Gobara, M., Baraka, A. (2014). Tartrazine solution as dosimeter for gamma radiation measurement. International Letters of Chemistry, Physics and Astronomy, 33: 106-117. https://doi.org/10.56431/p-b52d76

[5] Hadi, N.M., Hassan, A.F., Abaas, T.M. (2024). Nanomaterial mixed with dyes to make solar cell concentrator. Acta Innovations, 51: 29-35. https://doi.org/10.62441/ActaInnovations.51.5

[6] Jiang, D.F., Otitoju, T.A., Ouyang, Y., Shoparwe, N.F., Wang, S., Zhang, A.L., Li, S.X. (2021). A review on metal ions modified TiO_2 for photocatalytic degradation of organic pollutants. Catalysts, 11(9): 1039. https://doi.org/10.3390/catal11091039

[7] Jabbar, S.A., Mahdi, S.A., Naser, B.A. (2025). Nonlinear optical characteristics of Thin films made from mixed organic laser dyes doped with metal nanoparticles and PMMA polymer. Iraqi Journal of Applied Physics, 21(1): 121-126. https://doi.org/10.2025/qsctd988

[8] Leulescu, M., Rotaru, A., Pălărie, I., Moanţă, A., et al. (2018). Tartrazine: Physical, thermal and biophysical properties of the most widely employed synthetic yellow food-colouring azo dye. Journal of Thermal Analysis and Calorimetry, 134: 209-231. https://doi.org/10.1007/s10973-018-7663-3

[9] Li, M.X., Liang, X.L., Xie, P.Y., Zhang, C.Z., Chen, Y.H., Wang, C.Y., Zhou, L., Wang, T., Liu, H.X. (2024). Hierarchical porous structure design and water activation in hydrogels containing hyperbranched peach gum polysaccharide for efficient solar water evaporation. International Journal of Biological Macromolecules, 278: 134455. https://doi.org/10.1016/j.ijbiomac.2024.134455

[10] Lin, L.P., Zheng, Q.L., Chen, Q.S., Fang, M., Lai, Q.J., He, X.H., Qin, J.Y., Lin, Z.J., Lin, R.G. (2022). Preparation of fluorescent organic nanoparticles via self-polymerization for tartrazine detection in food samples. New Journal of Chemistry, 46(10): 4756-4761. https://doi.org/10.1039/D1NJ05176H

[11] Matinrad, F., Kompany-Zareh, M., Omidikia, N., Dadashi, M. (2020). Systematic investigation of the

measurement error structure in a smartphone-based spectrophotometer. Analytica Chimica Acta, 1129: 98-107..

[12] Patel, G.B. (2020). Study of optical, structural and dielectric properties of swift heavy ion irradiated biodegradable polymeric materials. Maharaja Sayajirao University of Baroda (India) ProQuest Dissertations & Theses.

[13] Patel, M. (2021). Understanding the electronic structure and electron transfer kinetics of titanium dioxide photoanodes and analyzing parameters affecting flatband potentials in metal oxides. Honors Thesis. https://doi.org/10.17615/14c3-xb93

[14] Siraj, N., El-Zahab, B., Hamdan, S., Karam, T.E., et al. (2016). Fluorescence, phosphorescence, and chemiluminescence. Analytical Chemistry, 88(1): 170-202.

[15] Ren, X.J., Wang, C., Wu, X., Rong, M.T., et al. (2024). Auxochrome dimethyl-dihydroacridine improves fluorophores for prolonged live-cell super-resolution imaging. Journal of the American Chemical Society, 146(10): 6566-6579. https://doi.org/10.1021/jacs.3c11823

[16] Rovina, K., Siddiquee, S., Shaarani, S.M. (2017). A review of extraction and analytical methods for the determination of tartrazine (E102) in foodstuffs. Critical Reviews in Analytical Chemistry, 47(4): 309-324. https://doi.org/10.1080/10408347.2017.1287558

[17] Banwell, C.N. (1972). Fundamentals of Molecular Spectroscopy. McGraw-Hill.

[18] Atkins, P., de Paula, J. (2017). Elements of Physical Chemistry. Oxford University Press.

[19] Ho, S.M. (2022). Investigation of optical properties of thin films by means of UV-visible spectrophotometer: A review. New Frontiers in Physical Science Research, 5: 66-82. https://doi.org/10.9734/bpi/nfpsr/v5/4498E

[20] Katariya-Jain, A., Deshmukh, R.R. (2022). Effects of dye doping on electro-optical, thermo-electro-optical and dielectric properties of polymer dispersed liquid crystal films. Journal of Physics and Chemistry of Solids, 160: 110363. https://doi.org/10.1016/j.jpcs.2021.110363